Polyether-Segmented Nylon Hemodialysis Membrane. VII. Studies on Surface Structures of Various Poly(ethylene oxide)-Segmented Nylon Membranes

AKIRA MOCHIZUKI,[1] KAZUHISA SENSHU,[1] YUKIO SEITA,[1] SHUZO YAMASHITA,[1] NAOTO KOSHIZAKI[2]

[1] Research and Development Center, Terumo Corporation, Inokuchi 1500, Nakaimachi, Ashigarakami-gun, Kanagawa 259-0151, Japan

[2] Department of Composite Material, National Institute of Materials and Chemical Research, Higashi 1-1, Tsukuba, Ibaraki 305-0046, Japan

Received 12 May 1999; accepted 26 August 1999

ABSTRACT: The relationships of the surface morphologies to the surface chemical compositions in poly(ethylene oxide)-segmented nylon (PEO–Ny) membranes prepared by the phase-inversion method were studied using scanning electron microscopy (SEM), electron spectroscopy for chemical analysis (ESCA), and static secondary ion mass spectrometry (SSIMS). The PEO–Ny's used were high semicrystalline PEO-segmented polyiminosebacoyliminohexamethylene (PEO–Ny610), low semicrystalline PEO-segmented poly(iminosebacoylimino-*m*-xylylene) (PEO–NyM10), and amorphous PEO-segmented poly(iminoisophthaloyliminomethylene-1,3-cyclohexylenemethylene) (PEO–NyBI). SEM observation showed that the surfaces of the PEO–Ny610 and PEO–NyM10 membranes were composed of crystalline spherulite and that the PEO–NyBI membrane surface had a nodular structure. ESCA analysis exhibited the enrichment of the PEO segment at the surfaces of the PEO–Ny610 and PEO–NyM10 membranes. On the other hand, the enrichment of the Ny segment was observed in the case of the PEO–NyBI membrane. SSIMS analysis revealed that the outermost surfaces of the PEO–Ny membranes except the PEO–NyBI membrane were almost covered with the PEO segment. © 2000 John Wiley & Sons, Inc. J Appl Polym Sci 77: 517–528, 2000

Key words: polyether-segmented nylon; membrane; phase inversion; surface structure; SEM; ESCA; SSIMS

INTRODUCTION

Many kinds of polymers have been synthesized and evaluated as biomedical materials. It is well known that some block copolymers exhibit good blood compatibility and have been applied to practical uses. Indeed, the surface structures of the polymers play a very important role in blood compatibility, and, thus, it is significant to know the surface structures of the block copolymers. Okano et al. evaluated the 2-hydroxyethyl methacryrate–styrene block copolymer in detail and they reported that the microphase-separated structure of the surface strongly affects blood compatibility and adhesion of the blood cell.[1,2] Yui et al. reported on the relationship between the surface structure and blood compatibility using poly(propylene oxide)-segmented nylon 610.[3,4]

We investigated the possibility of applying polyether-segmented nylon (PE–Ny) to a hemodialysis membrane and reported the permeability characteristics, the membrane morphologies, and

Correspondence to: A. Mochizuki.

Journal of Applied Polymer Science, Vol. 77, 517–528 (2000)

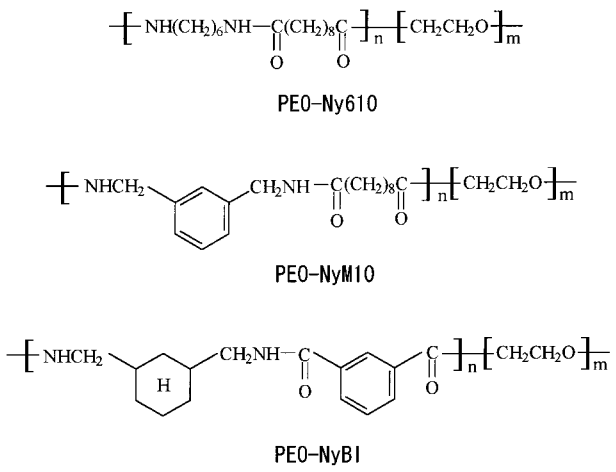

Figure 1 Chemical structures of PEO–Nys.

the blood compatibility for several kinds of membranes.[5–10] To produce a membrane, the phase-inversion method is usually adopted. This method is composed of four steps: The first step is the immersion of a polymer solution into a coagulant (nonsolvent). The second is the diffusion of the nonsolvent into the polymer solution and of the solvent into the coagulant. The third and the fourth are isothermal phase separation and precipitation of the polymer, respectively. Therefore, the coagulant composition plays a very important role in making a membrane structure. In this process, it is known that the morphology and permeation characteristics of the membrane are affected strongly by the coagulant composition.

As a block copolymer is composed of chemically different segments with different surface free energies, the surface chemical structure is affected by the environment of the surface. Thus, the phase-inversion method will produce a membrane with a quite different surface structure when an amorphous block copolymer is used as the membrane material. In a previous article, we reported the effect of coagulation conditions on the surface structure of the membranes prepared from amorphous PEO-segmented poly(iminoisophthaloyliminomethylene-1,3-cyclohexylenemethylene) (PEO–NyBI) using scanning electron microscopy (SEM), electron spectroscopy for chemical analysis (ESCA), and static secondary ion mass spectrometry (SSIMS).[10] The results indicate that the PEO segment affects the morphology and water permeability of the membrane and that the concentration of the PEO segment at the top surface depends on the coagulation condition. In this article, we report the surface morphologies and chemical structures for phase-inversion membranes made of three PEO–Ny's with different crystallinity using SEM, ESCA, and SSIMS. The segregation mechanism of the segment occurring at the PEO–Ny surface is also discussed.

EXPERIMENTAL

Materials

The abbreviations PEO–Ny610, PEO–NyM10, and PEO–NyBI stand for PEO-segmented polyiminosebacoyliminohexamethylene, PEO-segmented poly(iminosebacoylimino-*m*-xylylene), and PEO-segmented poly(iminoisophthaloyliminomethylene-1,3-cyclohexylenemethylene), respectively. The PEO–Ny's are multiblock copolymers, and their chemical structures are shown in Figure 1. The feed ratio of PEO was 10 wt % in the preparation of the copolymer. The molecular weights of the PEO segments were 2000 for PEO–Ny610 and PEO–NyM10 and 1000 for PEO–NyBI. The observed content and molecular weight of the PEO segment in PEO–Ny are summarized in Table I. PEO–Ny610 is a highly crystalline polymer (heat of crystalline fusion, ΔH = 55 J/g), and PEO–NyM10 is a low semi-crystalline polymer (ΔH = 30 J/g). The melting points of PEO–Ny610 and PEO–NyM10 are 220 and 189°C, respectively.[7] PEO–NyBI is an amorphous polymer and its glass transition point is 159°C.[10]

Preparation of PEO–Ny Membranes

The membranes were prepared according to the method described in previous articles.[6,10] The brief procedure is as follows: The semicrystalline PEO–Ny was dissolved in formic acid at 80°C, and amorphous PEO–NyBI was dissolved in DMSO at room temperature. The polymer solu-

Table I PEO Segment in PEO–Ny

Polymer	PEO content (wt %) Feed[a]	PEO content (wt %) Observed[b]	Molecular Weight of PEO
PEO–Ny610	10	10.6	2000
PEO–NyM10	10	10.2	2000
PEO–NyBI	10	9.8	1000

[a] Feed ratio in the preparation of PEO–Ny.
[b] Calculated from ^{1}H-NMR.

tion was cast onto a glass plate at room temperature (ca. 23°C), and the glass plate was immersed into ultrapure water as a coagulant for 1 h. Then, the membrane was kept in ultrapure water for over 24 h to remove the solvent and was preserved in pure water. The wet membrane was freeze-dried to analyze the surface structure.

SEM Observation

The wet membrane was immersed into liquid nitrogen. The frozen membrane was fractured in liquid nitrogen and then dried *in vacuo*. After spattering platinum onto the dry membrane, the surface was observed under a scanning electron microscope (SEM) equipped with a field emission gun at an accelerated voltage of 5 kV (JSM-840F, JEOL Ltd., Japan).

Measurement of ESCA and SIMS

The measurements of ESCA and SSIMS were performed according to the methods described in the previous article (PHI 5600ci, Perkin–Elmer).[10] The surface analysis by ESCA was carried out under the following conditions: The X-ray source was monochromatized Al Kα (1486.7 eV). The X-ray gun was operated at 14 kV and the anode power was 20 W. The base pressure was maintained at lower than 10^{-9} Torr. Pass energies of 187.5 and 29.25 eV were chosen for survey spectrum acquisition (0–1000 eV) and high-resolution spectrum acquisition (O1*s*, N1*s*, and C1*s*), respectively. The survey scan was carried out in order to survey the element species existing the surface. The photoelectron take-off angle (TOA) was 40° for PEO–Ny610 and PEO–NyM10 membranes, where the TOA was defined as the angle between the sample plane and the axis of the analyzer. This angle corresponds to about 7 nm of the sampling depth. The depth profile measurement was carried out for the PEO–NyBI membrane, where the TOAs were 10, 20, 40, and 75°. A low-energy electron flood gun (emission current: 0–20 mA; electron energy: 5–20 eV) was used to minimize sample charging. Quantification of the ESCA signals was performed by use of the software attached PHI 5600ci. All the binding energies were referenced by setting the CH_x peak maximum in the resolved C1*s* spectra to 285.0 eV.

The surface analysis by SSIMS was carried out as follows: The apparatus was the same one as for ESCA, a PHI 5600ci, equipped a quadruple mass analyzer. The Xe^+ ion of 3 keV was used as a primary ion and was rastered over a 3×1.5-mm^2 area with an average current density of 1 nA/cm^2. Charge neutralization was achieved with a low-energy flood gun. The sampling depth was about 1 nm.

RESULTS AND DISCUSSION

Surface Morphologies of Membranes

The surface morphologies of the PEO–Ny membranes were observed under SEM and the results are shown in Figure 2. The semicrystalline PEO–Ny610 and PEO–NyM10 membranes were prepared by the phase-inversion method using formic acid as a solvent and water as a coagulant. In the case of amorphous PEO–NyBI, DMSO and water were used as a solvent and a coagulant, respectively. It is known that in the phase-inversion process of a semicrystalline polymer solution the top surface of the membrane is composed of spherullite.[11] Figure 2(A) shows that the surface of the PEO–Ny610 membrane is composed of rather small and clear spherulites of 1–2-μm diameter. The small spherulites suggest that many crystalline nuclei formed and rapid crystallization occurred during the phase separation.

The PEO–NyM10 membrane gave a different result. Its top surface is composed of large but obscure spherulites of 5–10-μm diameter as shown in Figure 2(B). This surface structure suggests that slow crystallization occurs. In the phase-separation process of an amorphous polymer solution, a liquid–liquid phase separation with rapid precipitation usually occurs and then gives a membrane with a smooth surface.[12] As PEO–NyBI is amorphous, its morphology obtained by the phase-inversion process was expected to be the characteristic morphology of the common amorphous polymer membrane mentioned above, and, indeed, the smooth surface was observed at low magnification, $\times$5000 [Fig. 2(C)]. SEM observation at high magnification, $\times$50,000 [Fig. 2(D)], however, revealed that the surface is composed of fine nodules of 10–20-nm diameter. Many researchers have reported that the nodular structures can be observed at the top surfaces of ultrafiltration membranes and proposed the mechanisms of forming the nodular structure.[13–16] One of the likely mechanisms is spinodal demixing and it was discussed in detail by Wienk et al.[16] The formation mechanism of the surface structure for the PEO–NyBI membrane

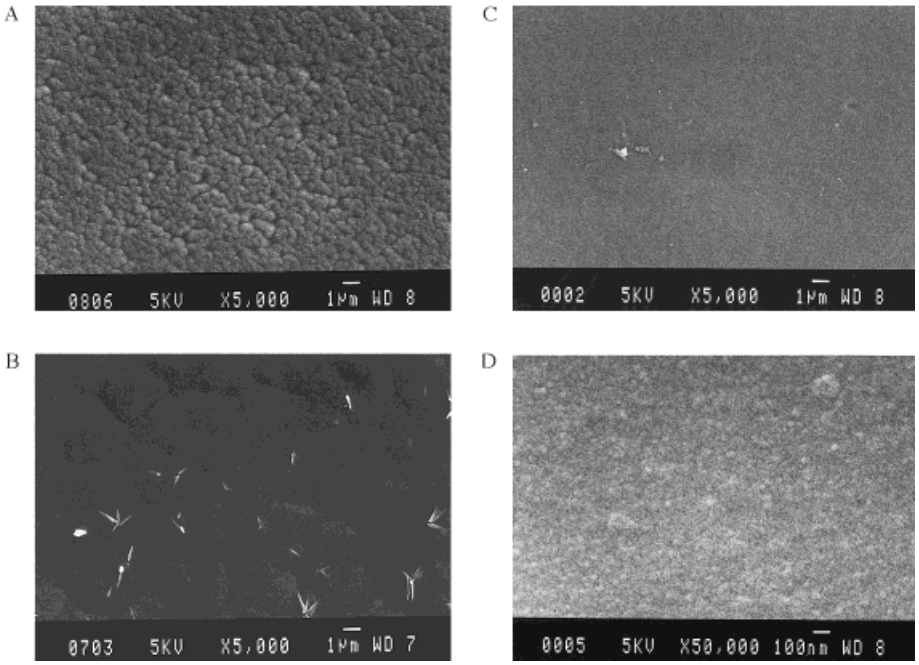

Figure 2 SEM pictures of top surfaces of PEO–Ny membranes. (A–C) Top surfaces of PEO–Ny610, PEO–NyM10, and PEO–NyBI membranes, respectively, and observed at magnification, ×5000. (D) Top surface of PEO–NyBI membrane observed at high magnification, ×50,000.

will be described below in terms of the surface analysis by ESCA.

Surface Compositions of Membranes

ESCA Analysis

The representative survey scan spectrum of ESCA is shown in Figure 3, where the sample is the PEO–Ny610 membrane, and the spectrum was recorded at a TOA of 40°. Quite similar spectra were obtained for the PEO–NyM10 and PEO–NyBI membranes except for the small difference of the peak intensity. These survey scans show that the elements detected are just only carbon, oxygen, and nitrogen and these results conclude that there is no contamination at the surfaces of all the samples. The experimental atomic compositions calculated from the peak intensities of the narrow scans are shown in Table II. The atomic ratios of oxygen observed in the PEO–Ny610 and PEO–NyM10 membranes are 17.3 and 17.9, respectively, while the theoretical values are 13.4% for PEO–Ny610 and 11.4 wt % for PEO–NyM10. These results reveal that the significant increase

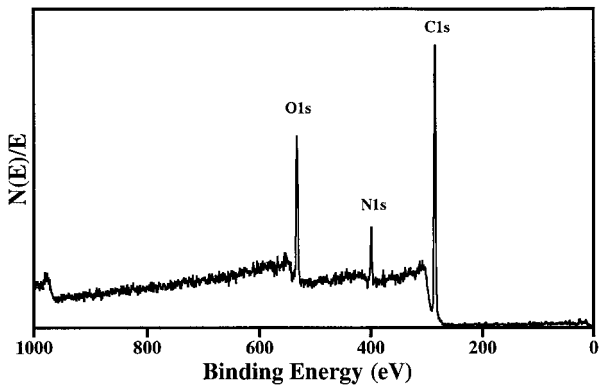

Figure 3 Typical survey scan spectrum of ESCA. Sample is PEO–Ny610 membrane.

Table II Experimental Atomic Ratio of Membrane Surface of PEO–Ny by ESCA

	Atomic Ratio[a] (%)		
Polymer	C	O	N
PPO–Ny610	75.6 (78.0)	17.3 (13.4)	7.1 (8.5)
PEO–NyM10	75.8 (80.4)	17.9 (11.4)	6.3 (8.2)
PEO–NyBI	78.8 (78.8)	12.3 (12.1)	9.0 (9.1)

[a] The values in the parentheses are theoretical ones.

of oxygen content at the top surface occurs in the semicrystalline PEO–Ny membranes. In the case of the PEO–NyBI membrane, no enrichment of the oxygen atom is observed. The observed and theoretical contents are 12.3 and 12.1%, respectively. At the same time, decrease of the nitrogen content is observed except for PEO–NyBI. The observed values are 7.1% for PEO–Ny610 and 6.3% for PEO–NyM10, and the theoretical ones are 8.5 and 8.2%, respectively. The observed nitrogen content in PEO–NyBI is almost equal to the theoretical one. The increase of the oxygen ratio and the decrease of the nitrogen ratio indicate the enrichment of the PEO segment at the top surface of the semicrystalline PEO–Ny membranes. On the other hand, the fact that the atomic ratio at the PEO–NyBI membrane surface is nearly equal to that of bulk PEO–NyBI indicates no or little enrichment of the PEO segment at the top surface of the membrane. It is well known that in amorphous block copolymers composed of hydrophilic and hydrophobic segments such as PEO–NyBI the enrichment of one segment at the top surface is observed. The phenomenon is governed by the interfacial free energy between the polymer and the circumstance, and the surface which minimizes the interfacial free energy is formed. Since in this study the PEO–NyBI membrane is prepared using water as a coagulant, the enrichment of PEO segment was easily anticipated because of the strong hydrophilicity of the PEO segment. However, the prediction does not agree with the result mentioned above.

Figures 4 and 5 show narrow scan spectra of carbon and oxygen signals, which were recorded at a TOA of 40° (ca. 7 nm of sampling depth). First, the carbon peaks are discussed: The existence of the three kinds of carbon peaks is predicted from the chemical structure of PEO–Ny as shown in Figure 1. One is of the carbons which link to the carbon (C—C) and/or hydrogen atom (C—H), and they appear at 285.0 eV. The second is of the carbons next to the ether oxygen (C—O) derived from the PEO segment and/or next to the amide nitrogen (C—NHCO), and they appear at 286.6 eV. The third is the carbon corresponding to the amide group of the Ny segment (NH—C═O) at 288.0 eV. One can notice clear differences among the shape of the carbon peaks of the PEO–Ny610, PEO–NyM10, and PEO–NyBI membranes. In the case of PEO–Ny610 and PEO–NyM10, the C—O/C—NHCO peak is observed as a large shoulder peak on the C—C/C—H peak. In addition, one can observe small peaks due to amide carbon (NH—C═O) in both spectra. On the other hand, the PEO–NyBI membrane has a significantly small C—O/C—NHCO peak as a shoulder peak and a broad peak due to the amide carbon at 288.0 eV. These results imply qualitatively that the significant enrichment of the PEO segment occurs at the top surfaces of the PEO–Ny610 and PEO–NyM10 membranes and little or no segregation takes place at the top surface of the PEO–NyBI membrane. When we try to quantify the chemical composition of the surface from

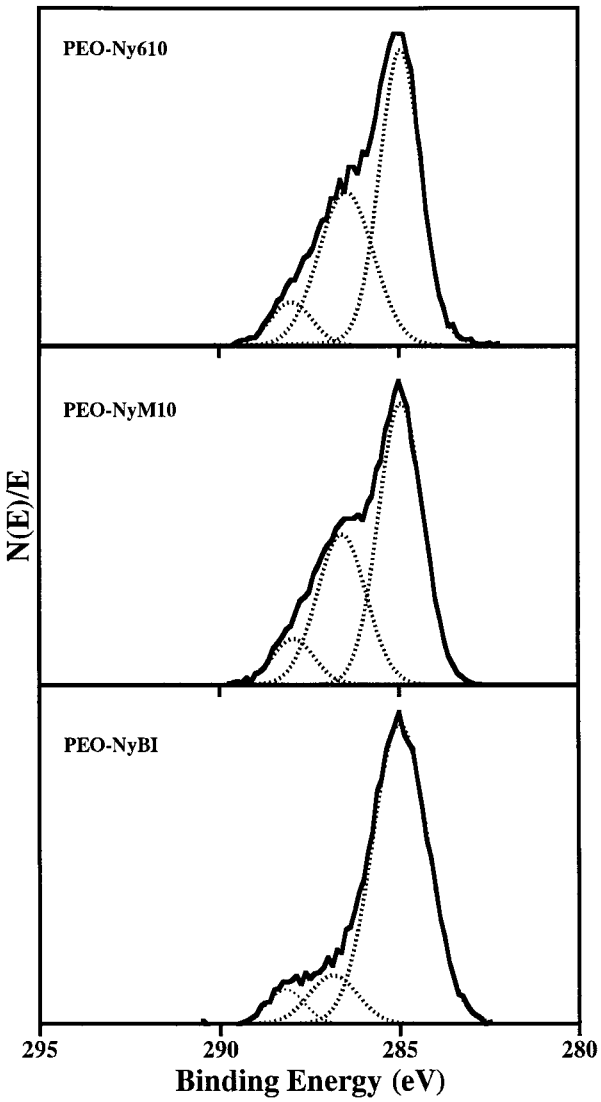

Figure 4 High-resolution ESCA spectra of carbon C1. The peak at 285.0 eV is assigned to hydrocarbon (C—C/C—H); the peak at 286.6 eV, to carbons linked to ether oxygen (C—O) or to amide nitrogen (C—NHCO); and the peak at 288.0, to amide carbon (NHC═O).

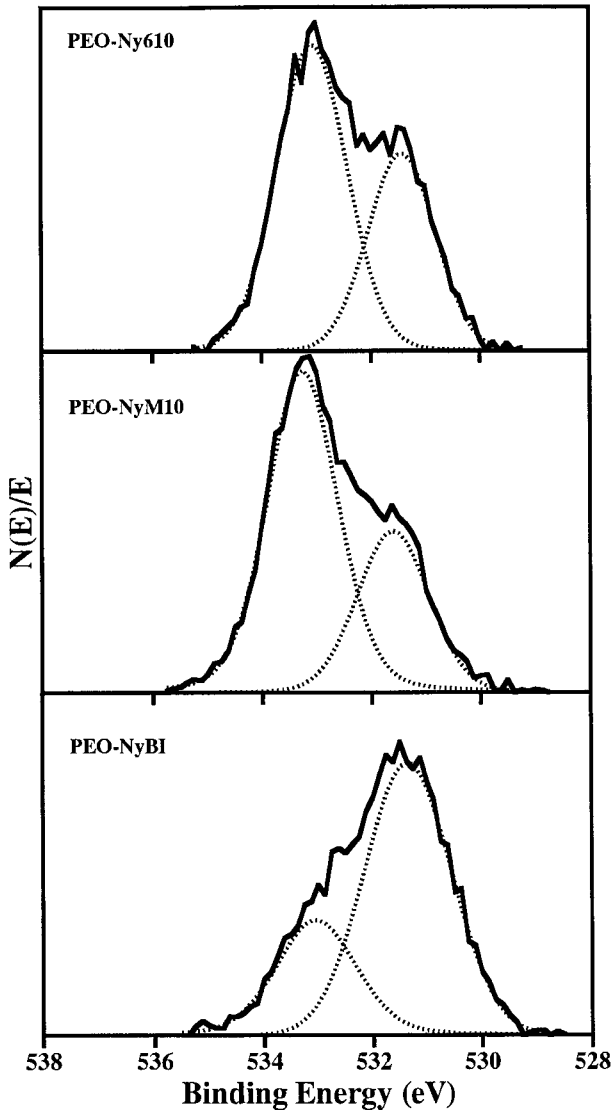

Figure 5 High-resolution ESCA spectra of oxygen O1*s*. The O1*s* peak can be resolved into two peaks: ether oxygen (O—C) at 531.5 eV and amide oxygen (NHC═O) at 531.5 eV.

the C1 peak, there are a large number of possible ways to curve-fit the peak into the three peaks. Moreover, we consider that C—O and C—NHCO have the same chemical shift and they cannot be curve-fitted into each peak. Consequently, we will get a result with a serious error of the estimation, so we did not analyze the carbon peaks to quantify the surface composition.

Next, the analysis of the oxygen, O1*s*, peak is described. The spectra of O1*s* derived from the three PEO–Ny's are shown in Figure 5. Although the O1*s* peak is a broad one with a shoulder, it can be curve-fitted into just two peaks easily without serious errors, because PEO–Ny has only two types of oxygen, as shown in the chemical structure of PEO–Ny (Fig. 1). The two peaks obtained by the curve-fitting are assigned to amide oxygen (NH—C═O) at 531.5 eV and ether oxygen (C—O) at 533.1 eV. The former is solely based on the amide group in the Ny segment, and the latter is based on the PEO segment. Consequently, the curve-fitted peaks will allow discrimination between the Ny and PEO segments. It is observed in the PEO–Ny610 and PEO–NyM10 membranes that the ether oxygen appears strongly as a main peak of O1*s* in spite of the low PEO content in the bulk copolymers. On the other hand, the ether oxygen peak is much smaller than is the amide oxygen peak in the PEO–NyBI membrane. The surface compositions of the membranes are calculated from the ratio of the two oxygen peaks, and the results are listed in Table III. The PEO contents at the top surfaces are 34, 37, and 12 wt % for PEO–Ny610, PEO–NyM10, and PEO–NyBI, respectively. These results lead to a conclusion that the marked enrichment of the PEO segment occurs especially in PEO–Ny610 and PEO–NyM10 and that in the case of the PEO–NyBI membrane surface the content of the PEO segment at the surface is equal to that in the bulk polymer. The result of the PEO–NyBI membrane is supported by the result from the atomic composition ratio at the top surface as mentioned above. The tendency observed in the semicrystalline PEO–Ny membranes coincides with the qualitative results from the C1*s* peak analysis mentioned above.

The enrichment of the PEO segment is described as follows: As PEO–Ny610 and PEO–NyM10 are semicrystalline polymers, the extrusion of the PEO segment from the spherulite will take place during the crystallization process of the Ny segment in phase inversion. This extrusion phenomenon was reported by Sangen et al.[17] They investigated the surface structure of the

Table III PEO Content at Top Surface of PEO–Ny Membrane

Membrane	PEO Content[a] (wt %)
PEO–Ny610	34
PEO–NyM10	37
PEO–NyBI	12

[a] Calculated from the ratio of ether oxygen (O—C) to amide oxygen (NH—C═O) in the ESCA spectra (TOA = 40°).

molten PEO-segmented poly(ethylene terephthalate) (PET) film, and the remarkable enrichment of PEO segment was observed. They attributed the phenomenon to the extrusion of the PEO segment from the crystalline phase during the rapid crystallization process of the PET segment.

Of course the minimization of the interfacial free energy between the polymer (PEO–Ny) and the environment (water) may contribute to constructing the surface structure. Considering that the PEO segment is strongly hydrophilic and that water is used as a coagulant in the membrane-formation process, the enrichment of the PEO segment at the top surface may be induced in order to minimize the interfacial free energy. The reason for no enrichment of PEO at the surface of the PEO–NyBI membrane can be explained by neither the extrusion mechanism nor the minimization of the interfacial free energy, because PEO–NyBI is an amorphous polymer. To interpret the result, the morphology of the membrane surface should be considered again.

In the section on SEM observation, it was described that the PEO–NyBI membrane surface is composed of the small nodules of 10–20-nm diameter. This nodule is the first aggregated particle of PEO–NyBI in the phase-inversion process. This size corresponds to the depth by which ESCA can survey with a 40° TAO (ca. 7 nm). Therefore, ESCA observed the composition of the whole nodule, and, consequently, the result of the surface analysis agrees with the bulk chemical composition of PEO–NyBI even if the segregation of one segment occurs at the nodule surface. In the case of the PEO–Ny610 and PEO–NyM10 membranes, the spherulite sizes are in the range of 1–10 μm, and this size is large enough for the sampling depth of ESCA.

The depth profile of the PEO–NyBI membrane surface was investigated to analyze the surface structure of the nodule, by changing the sampling depth from about 2 to 10 nm. The results are shown in Table IV, where the PEO contents at the top surfaces are calculated from the O1*s* oxygen peaks curve-fitted to two peaks, —C—O—C— and —NHC═O. The table exhibits that the decrease of the sampling depth brings about the decrease of the PEO content from 11 to 6.5 wt %. These results imply that the concentration of the Ny segment at the top surface of the PEO–NyBI membrane is higher than that of the bulk composition when the sampling depth becomes shallower. This observed result is opposite to the prediction of PEO enrichment from the interfacial free-energy theory. The reason for the enrichment of the Ny segment will be discussed below. The surface of the PEO–NyBI membrane has the nodular structure as mentioned above, and the formation process of the nodules will affect strongly the composition of the top surface.

Table IV Depth Profiling Result of PEO–NyBI Membrane by ESCA

TOA (Degree)	Theoretical Sampling Depth (nm)	PEO Content[a] (wt %)
75	9.4	11
40	6.4	12
20	3.4	6.5
10	1.7	6.5

[a] Calculated from the ratio of ether oxygen (O—C) to amide oxygen (NH—C═O).

The formation mechanism recently described on a molecular level by Wienk et al.[16] is useful to interpret this phenomenon. Their proposal is as follows: The polymer molecules make highly entangled coils in the high-concentration polymer solution such as a dope solution for membrane preparation. On immersing the polymer solution film into the coagulation bath, the rapid out-diffusion of the solvent and the in-diffusion of the nonsolvent occur and the polymer molecules are confronted with a noncompatible environment. Consequently, clustering of the polymer molecules into groups decreases the interaction of the polymer molecules with the nonsolvent. In the beginning of this process, the clusters are highly connected because some polymer molecules are entangled in adjacent clusters. Excess out-diffusion of the solvent increases the polymer concentration of the top layer and therefore results in the vitrification of the polymer matrix. Thus, the nodular structure is formed.

Considering this nodule formation mechanism, the enrichment of the Ny segment at the shallower top surface can be explained as follows: When the solubilities of PEO and Ny BI in DMSO are considered, it will be found that DMSO is a selective solvent, because PEO can dissolve little and NyBI can dissolve well in DMSO at room temperature. It is well known that the block copolymer in the selective solvent systems forms micelles with a corona and core structure, caused by the association of the insoluble block.[18–20] This indicates that the PEO–NyBI molecules in DMSO will give a heterogeneous solution due to forming

the concentration fluctuations or polymolecular micelles. In the solution, the PEO segments coalesce each other to diminish the interactions with the poor solvent, DMSO, and they are surrounded by Ny segments which entangle in other Ny segments. By means of forming such a structure, the polymer solution will remain in the stable state. This heterogeneous structure will correspond to the cluster in the Wienk's proposal. On immersing the PEO–NyBI solution film into water, the rapid out-diffusion of DMSO and in-diffusion of water set in and the aggregation of the Ny segment starts to diminish the interactions of the Ny segment with the nonsolvent. Thus, the PEO segment will be confined to the inner side of the cluster by the Ny segment, and the nodule with the Ny segment-rich surface is formed.

SSIMS Analysis

SSIMS analysis was carried out to investigate the structure of the outermost surface of the PEO–Ny membranes. SSIMS can analyze a shallower surface structure within about 1 nm of the depth and can give chemical information on the surface structure from the fragmentation pattern of the polymer or segment constituting the surface. The positive MASS spectra of the homopolymers, PEO, Ny610, NyM10, and NyBI, are shown in Figure 6, where solvent-cast films from a hexafluoroisopropanol solution were used. They are the references for analyzing the surface structures of the PEO–Ny610, PEO–NyM10, and PEO–NyBI membranes. Since Ny610, NyM10, and NyBI are homopolymers, it is assumed that the surface structures are not affected by the sample preparation method.

The main ion structure assignments of the positive SIMS spectra in a high mass range for PEO, Ny610, NyM10, and NyBI are summarized in Tables V–VIII. In comparing the fragmentation pattern of PEO with those of the Nys in Figure 6, one can notice the following facts: The peak at $m/z^+ = 45$ with high intensity is detected in the PEO fragmentation, but not detected in the Ny fragmentations. This peak is assigned as $^+CH_2CH_2$—OH. On the other hand, the peak at $m/z^+ = 100$ in the Ny610 spectrum, the peak at $m/z^+ = 119$ in NyM10, and the peak at $m/z^+ = 105$ in Ny BI with high intensities are not detected in the PEO spectrum. These peaks are assigned as $^+CH_2$—$(CH_2)_3$—CO—NH_2 (Ny610), H_2C—Ph—$CH{=}NH_2^+$ (NyM10), and · Ph—C≡O^+ (NyBI), respectively.

The spectra of the PEO–Ny610, PEO–NyM10, and PEO–NyBI membranes are shown in Figure 7. The spectra of the PEO–Ny610 and PEO–NyM10 membranes show that the fragmentation patterns are very similar to that of PEO homopolymer although some small peaks are observed in the range from $m/z^+ = 90$ to $m/z^+ = 150$ derived from the fragmentation of the Ny segment. These results indicate qualitatively that the outermost surfaces of the PEO–Ny610 and PEO–NyM10 membranes are covered with the PEO segment. The outermost surface compositions of the PEO–Ny610 and PEO–NyM10 membranes observed by SSIMS are highly enriched with the PEO segment in comparison with the surface compositions observed by ESCA with the TOA = 40°. ESCA analyses reveal clearly the existence of the Ny segment at the top surface as described above. The reason for the discrepancy is attributed to the difference of the sampling depth. SSIMS can analyze the very outermost surface of the sample within about 1 nm of the depth, while ESCA analyzes within about 7 nm (TOA = 40°) in this experiment.

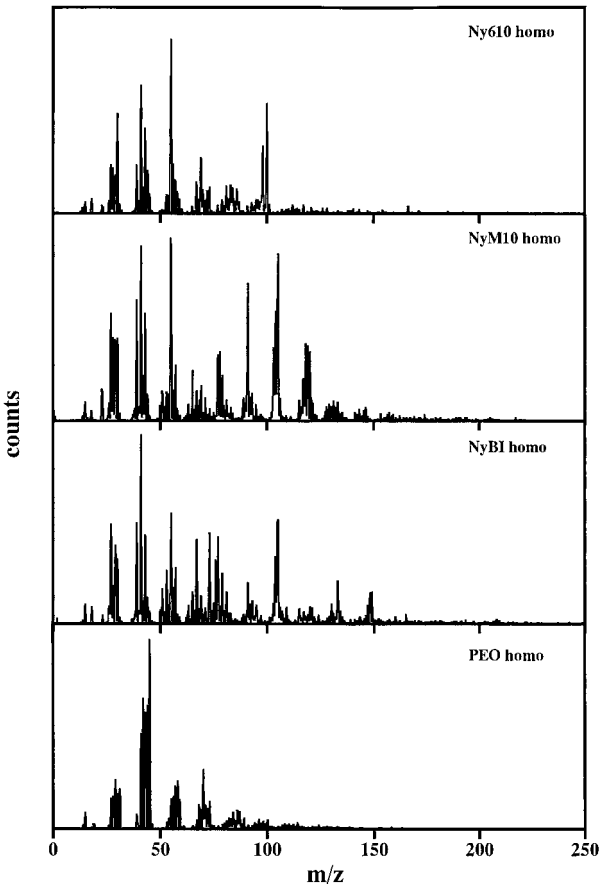

Figure 6 Positive SSIMS spectra of homopolymer films. Films were prepared by solvent-cast method.

Table V Assignment of Main Cation Peaks in the SIMS Spectrum of Ny610

m/z	Structure
30	$CH_2{=}NH_2^+$
41	$CH_2{=}CH{-}CH_2^+$
55	$CH_2{=}CH{-}C{\equiv}O^+$
69	$CH_3{-}CH_2{-}CH{=}CH{-}CH_2^+$
98	$^+CH{=}CH{-}(CH_2)_2{-}C(=O){-}NH_2$
100	$^+CH_2{-}(CH_2)_3{-}C(=O){-}NH_2$
166	$CH_2{=}CH{-}(CH_2)_4{-}NH{-}C(=O){-}CH_2{-}CH{=}CH^+$

For a more quantitative discussion, the peak intensity ratios of the Ny's characteristic peak to PEO's peak ($m/z^+ = 45$) in the spectra of the PEO–Ny's are taken. The peak ratio for each PEO–Ny sample is listed in Table IX. The ratios of the PEO–Ny610 and PEO–NyM10 membranes are 1.1×10^{-1} and 6.9×10^{-3}, respectively, and they are significantly small. These remarkable enrichments of the PEO segments are attributed to the same reasons as described in the discussion of the ESCA results, that is, the main reason is the extrusion of PEO segments from the spherulite.

In comparing the spectrum of the amorphous PEO–NyBI membrane with those of the semicrystalline PEO–Ny membranes, one can find easily the difference of the fragmentation patterns among them. The fragments based on the NyBI segment are clearly observed in the high mass range from $m/z = 100$ to $m/z = 150$, and the fragmentation pattern resembles that of homo-NyBI. This result supports the depth-profiling results of the PEO–NyBI membrane by ESCA as described above.

In a previous article, we investigated the effect of the coagulant composition on the surface struc-

Table VI Assignment of Main Cation Peaks in the SIMS Spectrum of NyM10

m/z	Structure
27	$CH_2{=}CH_2^+$
41	$CH_2{=}CH{-}CH_2^+$
55	$CH_2{=}CH{-}C{\equiv}O^+$
77	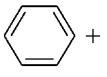
91	
105	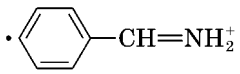
119	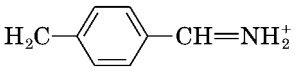

Table VII Assignment of Main Cation Peaks in the SIMS Spectrum of NyBI

m/z	Structure
27	$H_2C{=}CH^+$
41	$H_2C{=}CH{-}CH_2^+$
55	$H_2C{=}CH{-}C{\equiv}O^+$
77	
91	
104	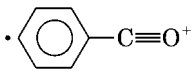
105	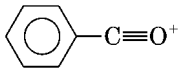
133	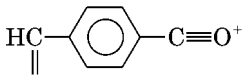
148	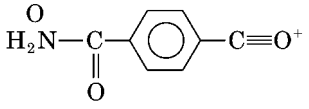

Table VIII Assignment of Main Cation Peaks in the SIMS Spectrum of PEO

m/z	Structure
15	CH_3^+
31	$^+H_2C—OH$
45	$^+H_2C—H_2C—OH$
73	$CH_3 \cdot CH_2—O—CH_2—CH_2^+$

Table IX Surface Structure of PEO–Ny Membrane by SSIMS

	m/z^+ of Fragment		
Membrane	Ny (*a*)	PEO (*b*)	Count Ratio[a]
PEO–Ny610	100	45	1.0×10^{-1}
PEO–NyM10	119	45	6.9×10^{-3}

[a] The count ratio is the peak intensity ratio of *a* to *b*.

ture of the PEO–NyBI membrane using water/DMSO mixed solutions as coagulants.[10] In the article, it was reported that the surface compositions of the membranes observed by ESCA (TOA = 40°) had been almost equal to the bulk composition of the PEO–NyBI polymer and that the qualitative increase in the content of the NyBI segment at the outermost surface of the membrane was observed by SSIMS with an increase of DMSO concentration in the coagulant. The results reported are shown in Table X.[10] These phenomena were discussed from the viewpoint that the binodal decomposition had contributed to constructing the surface structure. In this study, however, we observed the top surface of the PEO–NyBI membrane under SEM at high magnification and found a nodular structure with the diameter of about 10–20 nm. Moreover, the depth profile of ESCA revealed the enrichment of the NyBI segment at the shallower surface of the PEO–NyBI membrane, as described above.

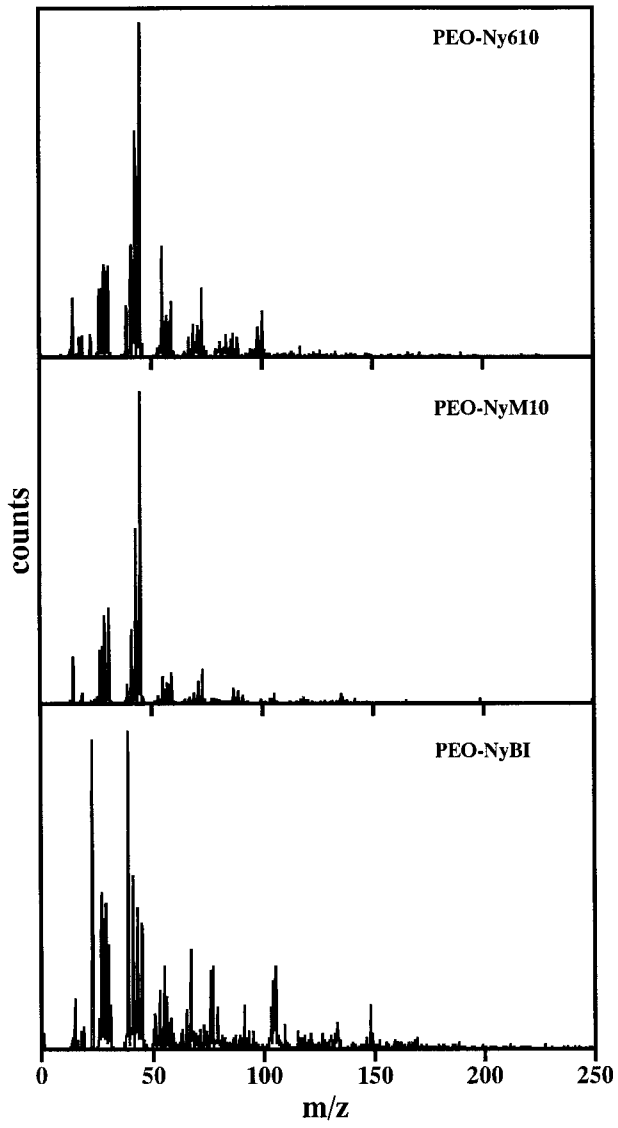

Figure 7 Positive SSIMS spectra of PEO–Ny membranes.

From these results, it is more suitable to discuss the previous results in terms of the formation process of the nodule, that is, the effect of the DMSO concentration in the coagulant on the surface composition of the PEO–NyBI membrane can be explained by the dope structure of PEO–NyBI or the clustering model of the polymer molecule according to Wienk's proposal[16] as described in the section on ESCA. When PEO–NyBI dissolves in DMSO, the solution will have a heterogeneous structure with concentration fluctuation or polymolecular micelles, where the PEO segments will coalesce each other to diminish the interaction with DMSO and will be surrounded by the Ny segment as mentioned above. On immersing the polymer solution film into the coagulant, the aggregation of the NyBI segment sets in to diminish the interaction with the nonsolvent (water) and the polymer is vitrified. The increase of the DMSO concentration in the coagulant delays the start of the aggregation of the NyBI segment because of the slow in-diffusion of water into the polymer solution film. This delay will change the heterogeneous structure. The increase of water content in the polymer solution film by the in-diffusion of water changes the solubility strength

Table X Effect of Coagulant Composition on Surface Structure of PEO–NyBI Membrane[10]

Coagulant Composition Water/DMSO (wt/wt)	Count Ratio[a] ($m/z^+ = 105 : m/z^+ = 45$)
100 : 0	0.66
80 : 20	0.54
60 : 40	0.52
40 : 60	0.30

[a] The count ratio is peak intensity ratio of NyBI to PEO segments in the SSIMS spectrum of the PEO–NyBI membrane. The fragment peaks, $m/z^+ = 105$ and $m/z^+ = 45$, were derived from the Ny segment and the PEO segment, respectively.

of the solvent constituting the dope solution continuously from a selective solvent (for NyBI segment) to a common solvent and, moreover, to another specific solvent (for PEO segment). According as the coagulant composition change, the solution structure will be rearranged, and the reverse structure, where the Ny segments coalesce each other and are surrounded with PEO segments, will be finally formed in order to minimize the interaction between the mixed solvent and the polymer. On the other hand, vitrification sets in when the water content in the polymer solution film reaches a certain content. The rearrangement competes with the vitrification kinetically. The rapid in-diffusion of water causes the aggregation with little or no rearrangement of the solution structure and enough delay of the coagulation brings about the rearrangement. Thus, the content of PEO segments at the top surface of the PEO–NyBI membrane increases with increasing DMSO content in the coagulant.

CONCLUSIONS

The surface structures of membranes made of three kinds of PEO-segmented nylon multiblock copolymers were investigated using SEM, ESCA, and SSIMS. The block copolymers used were high semicrystalline PEO–Ny610, low semicrystalline PEO–NyM10, and amorphous PEO–NyBI. The membrane was prepared by using a phase-inversion process. It was found by the SEM observation that the top surfaces of the PEO–Ny610 and PEO–NyM10 membranes were composed of the spherulite. In the case of the PEO–NyBI membrane, a smooth top surface was observed under SEM at low magnification and a nodular structure was observed at the top surface at high magnification. The ESCA analysis revealed that the top surfaces of the PEO–Ny610 and PEO–NyM10 membranes were significantly enriched with PEO segments. This result is explained by the extrusion of the PEO segment from the spherulite in the crystallization process of the Ny segment. In the PEO–NyBI membrane, the enrichment of the Ny segment was observed by ESCA analysis. This unexpected result is explained in terms of the formation process of the nodule, which constitutes the top surface of the membrane. The SSIMS analysis supported the results of ESCA and revealed that there was no or little Ny segment at the outermost top surfaces of the semicrystalline PEO–Ny membranes except that of the PEO–NyBI membrane. The fragmentation pattern of the PEO–NyBI membrane was similar to that of the homo-NyBI.

The authors thank T. Nakazaki, T. Fukuoka, and K. Matsushima for their help with the synthesis of the PEO-segmented nylons and Y. Inomata for her assistance with the ESCA measurement. We also would like to thank Dr. N. Yui (Japan Advanced Institute of Science and Technology, Japan), Dr. N. Ogata (Chitose Institute of Science and Technology, Japan), Dr. K. Kataoka (The University of Tokyo, Japan), Dr. T. Okano (Tokyo Women's Medical College, Japan), and Dr. Y. Sakurai (Tokyo Women's Medical College, Japan) for their helpful discussion.

REFERENCES

1. Okano, T.; Aoyagi, T.; Kataoka, K.; Abe, K.; Sakurai, Y.; Shimoda, M.; Shinohara, I. J Biomed Mater Res 1986, 20, 919.
2. Okano, T.; Suzuki, K.; Yui, N.; Sakurai, Y.; Nakahama, S. J Biomed Mater Res 1993, 27, 1519.
3. Yui, N.; Sanui, K.; Ogata, N.; Kataoka, K.; Okano, T.; Sakurai, Y. Jpn J Art Org 1981, 10, 1070.
4. Takei, Y.; Yui, N.; Maruyama, A.; Sanui, K.; Sakurai, Y.; Ogata, N. J Biomater Sci Polym Ed 1994, 6, 149.
5. Seita, Y.; Mochizuki, A.; Nakagawa, M.; Takanashi, K.; Yamashita, S. J Appl Polym Sci 1997, 65, 1703.
6. Mochizuki, A.; Seita, Y.; Endo, F.; Saiga, N.; Yamashita, S. J Appl Polym Sci 1997, 65, 1713.
7. Mochizuki, A.; Seita, Y.; Nakazaki, T.; Fukuoka, T.; Matsushima, K.; Yamashita, S. J Appl Polym Sci 1997, 65, 1723.
8. Mochizuki, A.; Seita, Y.; Saiga, N.; Yamashita, S. J Appl Polym Sci 1997, 65, 1731.

9. Mochizuki, A.; Seita, Y.; Nakashima, T.; Endo, F.; Yamashita, S. J Appl Polym Sci 1998, 67, 1253.
10. Mochizuki, A.; Senshu, K.; Seita, Y.; Fukuoka, T.; Yamashita, S.; Koshizaki, N. J Appl Polym Sci 1998, 69, 1645.
11. Cheng, L.-P.; Dwan, A.-H.; Gryte, C. J Polym Sci Part B Polym Phys 1995, 33, 211.
12. Boom, R. M.; Wienk, I. M.; van den Boomgaad, T.; Smallders, C. A. J Membr Sci 1992, 73, 277.
13. Kesting, R. E. J Appl Polym Sci 1990, 41, 2739.
14. Broens, L.; Altena, F. W.; Smolders, C. A.; Koenhen, D. M. Desalination 1980, 32, 33.
15. Ray, R. J.; Krantz, W. B.; Sani, R. L. J Membr Sci 1985, 23, 155.
16. Wienk, I. M.; van den Boomgaad, T.; Smallders, C. A. J Appl Polym Sci 1994, 53, 1011.
17. Sangen, O.; Kumeno, M.; Yamasaki, H.; Nakano, H.; Yamana, K. Kobunshi Ronbunshu 1992, 49, 459.
18. Block Polymers; Aggarwal, S. L., Ed.; Plenum: New York, 1970.
19. Ceresa, R. J. J Polym Sci C 1969, 26, 201.
20. Zhang, L.; Eisenberg, A. Polym Adv Technol 1998, 9, 677.